INTERNATIONAL JOURNAL OF CLIMATOLOGY
Int. J. Climatol. (2015)
Published online in Wiley Online Library
(wileyonlinelibrary.com) DOI: 10.1002/joc.4543

RMetS
Royal Meteorological Society

Spatiotemporal characteristics of hourly precipitation over central eastern China during the warm season of 1982–2012

Deshuai Li,[a] Jianhua Sun,[b,c]* Shenming Fu,[b] Jie Wei,[b] Shigong Wang[d] and Fuyou Tian[e]

[a] *College of Atmospheric Sciences, Lanzhou University, China*
[b] *Institute of Atmospheric Physics, Chinese Academy of Sciences, Beijing, China*
[c] *Collaborative Innovation Center on Forecast and Evaluation of Meteorological Disasters, Nanjing University of Information Science & Technology, China*
[d] *College of Atmospheric Sciences, Chengdu University of Information Technology, China*
[e] *National Meteorological Center, China Meteorological Administration, Beijing, China*

ABSTRACT: An intensive observational hourly precipitation data set from the China Meteorological Administration was utilized to investigate the changes in precipitation amount, frequency, intensity and duration over central eastern China during the warm season from 1982 to 2012. Ten intensity categories were used to reveal the contributions of precipitation frequency and intensity to the variation of rainfall amount. Moreover, the trends of frequency were also evaluated by comparing the respective contributions of the number and the duration of precipitation events. The main results are as follows: (1) The precipitation amount and intensity both decreased from southeast to northwest China, with two areas of high precipitation frequency located in southwestern and southeastern China. A region of high precipitation duration was found in central China and two lower duration regions were found in southern and northern China. (2) Generally, the extreme heavy rainfall showed a significant increasing trend while the light rainfall showed a significant decreasing trend over central eastern China. Nevertheless, the spatial unevenness was detected and in south and southeast China, significant increasing trends were found, whereas in northeast China and the Sichuan Basin, precipitation amounts showed a declining trend in each precipitation intensity category. (3) The trends of precipitation amount were mainly caused by the variations of precipitation frequency, which had a contribution rate of greater than 95%; however, for the heavy rainfall category, intensity changes were also very important. (4) Increased precipitation frequency was largely caused by the prolonged duration of rainfall events, whereas the decreased frequency was mainly due to the reduction in the number of rainfall events.

KEY WORDS hourly precipitation; trends; intensity; frequency; duration; central eastern China

Received 15 March 2015; Revised 6 September 2015; Accepted 23 September 2015

1. Introduction

Climate change is closely related to variations in the local total accumulated precipitation amount, but changes in intensity, frequency and duration are also very important to the environment and society. For instance, steady moderate rains soak into the soil and benefit plants, whereas the same rainfall amount over a short period of time may cause local flooding and runoff, leaving soils much drier after the event (Trenberth *et al.*, 2003). As a key component of the hydrological cycle, the variation in precipitation could determine the distribution of water resources, which is closely related to flood and drought regions, especially in vulnerable areas. Under the influence of the East Asian summer monsoon, central eastern China, which is densely populated and highly developed economy, often suffers from flood or drought events that are caused by the variation in precipitation, particularly in the warm season (from May to September).

Over the past few decades, substantial evidence has confirmed that extreme precipitation has experienced significant changes worldwide (Karl and Knight, 1998; Kiktev *et al.*, 2003; Zhai *et al.*, 2005; Allan *et al.*, 2010; Zhang *et al.*, 2011b; Donat *et al.*, 2013; O'Gorman, 2015; Trenberth *et al.*, 2015). Increasing trends of extreme rainfall during the past several decades are detected over most continents in a warmer climate based on daily precipitation data (Alexander *et al.*, 2006; Min *et al.*, 2011).

However, precipitation extremes increase faster than calculated by the Clausius–Clapeyron rate ('super CC rate') has also been found (Lenderink and Van Meijgaard, 2008; Berg *et al.*, 2009; Hardwick-Jones *et al.*, 2010; Utsumi *et al.*, 2011; Berg and Haerter, 2013; Molnar *et al.*, 2015), and the maximum daily precipitation showed distinct meridional variations with the greatest sensitivity in the tropics and higher latitudes for climate changes (Westra *et al.*, 2013; Asadieh and Krakauer, 2015). Additionally, these trends are further studied at sub-daily time scale, and the results show that the time scales and convective/stratiform systems of rainfall events generally have strong influence on the relationship between the extreme rainfall intensity and temperature (Haerter and Berg, 2009; Haerter *et al.*, 2010; Utsumi *et al.*, 2011; Westra and

* Correspondence to: J. Sun, Laboratory of Cloud-Precipitation Physics and Severe Storms, Institute of Atmospheric Physics, Chinese Academy of Sciences, Hua-Yan-Li No. 40, Beichen West Street, Chaoyang District, P.O. Box 9804, Beijing 100029, China. E-mail: sjh@mail.iap.ac.cn

Sisson, 2011; Berg *et al.*, 2013), and there was also a link between extreme rainfall duration and season (Zheng *et al.*, 2015).

For changes in temporal distribution of precipitation in different regions, there are two distinct patterns in observations: the first is 'more heavy and light precipitation while less moderate precipitation', such as in western Europe and the United States (Rajah *et al.*, 2014); the other pattern is 'increasing in heavy rainfall days at the expense of moderate and/or light rainfall days', such as in East Asia (Liu *et al.*, 2005; Trenberth, 2011; Wen *et al.*, 2014). In the United States, the precipitation amount generally increased by about 10% during 1910–1996 (Karl and Knight, 1998), but a less uniform distribution of precipitation was also found during wet days and among different regions (Kunkel *et al.*, 2003; Groisman *et al.*, 2005; Groisman *et al.*, 2012; Rajah *et al.*, 2014). While in Japan, the differential precipitation trends were characterized by increasing at high categories and decreasing at low categories (Fujibe *et al.*, 2005). In Singapore, the yearly rainfall totals as well as the hourly and daily precipitation extremes increased, and the increase in daily extremes was the fastest (Beck *et al.*, 2015). In India, the trends of the extreme hourly heavy rainfall events differed among seasons, and in summer, an increasing trend was significant, whereas in winter the trend was very weak (Sen Roy, 2009). Furthermore, climate models predicted that extreme heavy precipitation will increase under global warming and precipitation trends may become more spatially heterogeneous (Voss *et al.*, 2002; Kunkel *et al.*, 2003; Lau *et al.*, 2013; Sillmann *et al.*, 2013).

Over the mainland of China, the annual mean precipitation featured no significant variation during 1951–2000, but regional and seasonal variations were very obvious (Liu *et al.*, 2005; Zhai *et al.*, 2005; Yao *et al.*, 2008; Yu *et al.*, 2010). Regionally, precipitation increased in southeast and northwest China but decreased in the middle and northeast parts. Seasonally, precipitation increased during winter and summer but decreased during spring and autumn. When considering precipitation intensity, an overall negative trend in the frequency of light precipitation events and a positive trend in the frequency of extreme precipitation events have been found (Qian *et al.*, 2007; Huang and Wen, 2013; Wen *et al.*, 2014). The interannual variability of rainfall has also been investigated (Yang *et al.*, 2013), revealing that most of the climate change points occurred in the 1980s, which was consistent with the rapid development period of the economy in China.

However, there remains significant uncertainty related to the trends of hourly precipitation, because rainfall events often last for only a few hours per day and sometimes even for less than one hour, so the conclusions from daily-scale studies could not be used to the sub-daily time scale directly (Trenberth, 1998; Trenberth *et al.*, 2003; Westra *et al.*, 2014). Most previous studies mainly focused on daily or extreme precipitation events, while we will emphasize the changes in precipitation characteristics (amount, frequency and intensity) in each category in this article. Moreover, the question that how much of any precipitation changes is attributable to variations in rainfall frequency versus intensity over China is still not clear. On the basis of previous studies, the purpose of this article is to evaluate the changes in hourly precipitation in China by using an intensive hourly precipitation data set, and to separate and compare the respective contributions of the frequency and intensity trends to the total precipitation trend, which is critical in understanding changes in the hydrological cycle and can help us to obtain additional insight into these processes.

The remainder of the article is structured as follows. The data and methods are described in the next section. The geographic distribution of precipitation features and regional trends of precipitation and frequency are shown in Sections 3 and 4, respectively. Finally, a conclusion is presented in Section 5.

2. Data and methods

2.1. Data

In this study, the intensive hourly precipitation data set was obtained from the National Meteorological Information Centre (NMIC) of the China Meteorological Administration, which includes a total of 2420 stations and covers the entire warm season (May–September) from 1982 to 2012. Compared with the sub-daily data set such as the HadISD (Dunn *et al.*, 2012; Westra *et al.*, 2014), the hourly data from the NMIC is much more complete and can give more detailed information. In addition, although hourly precipitation data are available from 1951, there are many unreliable and missing data from most stations before 1982, hence the period 1982–2012 was selected. The daily precipitation data set over China, which includes a total of 839 stations, was used to validate the hourly precipitation data set. The hourly precipitation data were recorded automatically using tipping-buckets or siphon rain gauges, and daily precipitation was recorded through manual observations at 6-h intervals. It should be noted that these two precipitation data sets have already undergone strict quality control, including an extreme value test for climate background and a time consistency and internal consistency check (Yu *et al.*, 2007a; Li *et al.*, 2011).

To minimize the biases introduced by the presence of missing data, further quality control has been applied. According to Zhai *et al.* (2005) and Karl and Knight (1998), each station had to preserve at least 80% of the total data series. Furthermore, Kunkel *et al.* (2003) and Villarini *et al.* (2013) used the stations with a proportion of missing data lower than 10% of the total length. In this analysis, two strict quality control conditions have been adopted: (1) for the hourly precipitation data, the missing data must be less than 2% of the total data series and (2) for the daily precipitation data, the data series should be 100% complete during the analysis timeframe. After this procedure, a total of 1141 stations for the hourly data (47.1%) and a total of 820 stations for the daily data (97.7%) were retained for the subsequent analyses. The daily data stations are fairly evenly distributed in the areas to the east

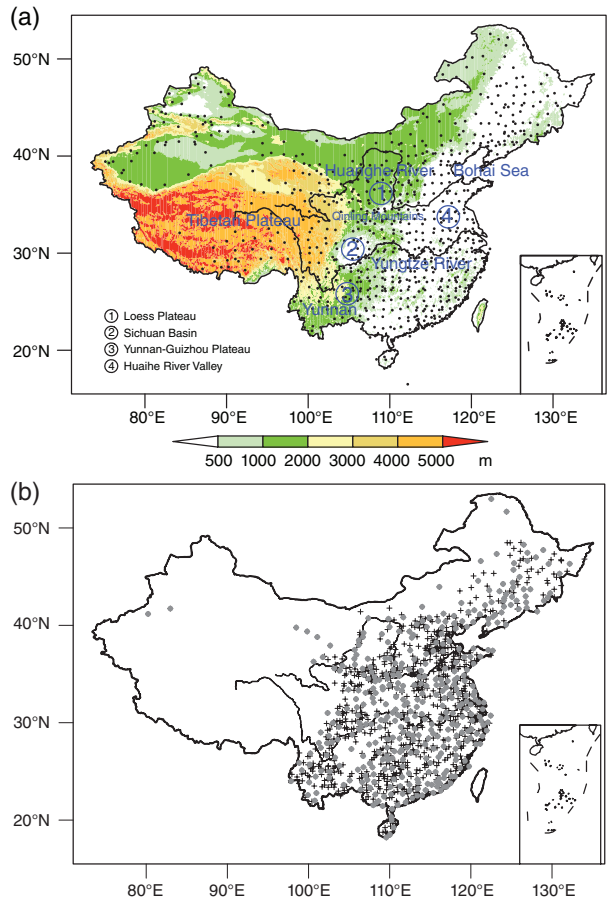

Figure 1. Distributions of the daily (a) and hourly (b) stations used in this study, with symbols '·' and '+' both represent the locations of precipitation stations, and the gray dots represent coincident stations of daily and hourly data set. The shading colors denote altitude (units: m).

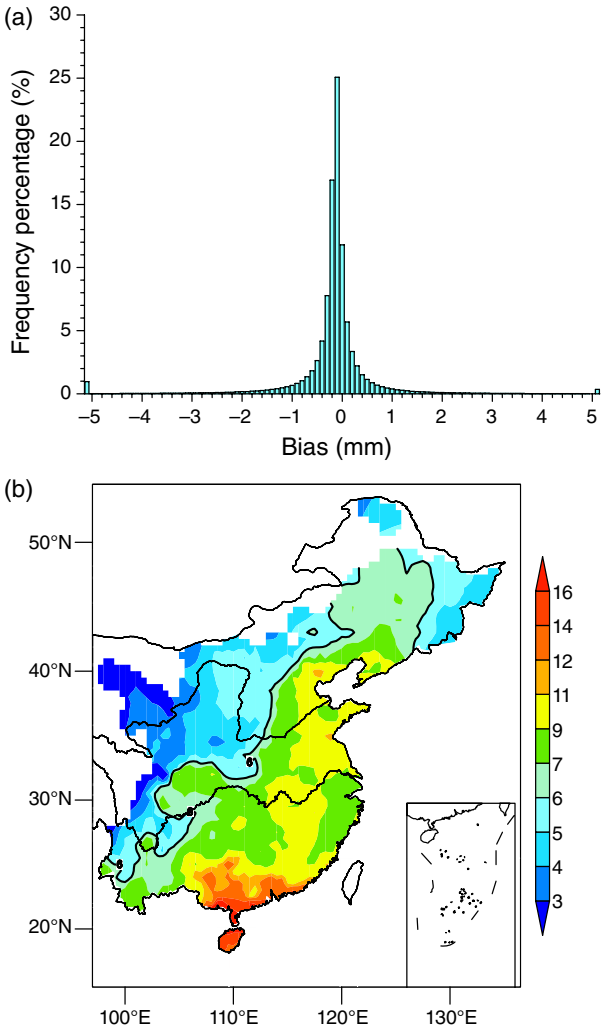

Figure 2. Frequency percentage of the bias between 24-h total accumulated amount of hourly precipitation and daily precipitation records (a) and the 95th percentile of hourly precipitation (b, units: mm h^{-1}).

of 95°E (Figure 1(a)), whereas the hourly data stations are mainly located over central eastern China (Figure 1(b)). The stations in which both daily and hourly precipitation data were recorded are shown by the gray dots in Figure 1(b). From these stations, the daily data set can be used as a reliable reference to validate the hourly data sets. As Figure 1(b) illustrates, there are 288 stations in which both data sets are recorded and are mainly located in central eastern China. For each one of these stations, it is possible to convert the hourly precipitation into the daily accumulated precipitation and obtain the bias between them as follows:

$$dr = \sum_{h=1}^{24} R_h - R_d \qquad (1)$$

where R_h represents the hourly data records and R_d is the corresponding daily rainfall. Figure 2(a) shows the frequency percentage of the bias with an increment of 0.1 mm h^{-1}, from which it is clear that most of the bias was between −1.0 and 1.0 mm with the accumulated contribution exceeding 90%. Bias between 0.5 and 5.0 mm accounted for 19.1% of the accumulated contribution; however, only 1.3% exceeded 5 mm. Overall, the bias obeys the normal distribution, which implies that the hourly precipitation data does not feature a systematic bias. Therefore, the 2% of hourly data that is missing from the total time series should have minimal impact on our results and the data are considered reliable.

2.2. Methods

As the hourly data were used, precipitation frequency was defined as the number of hours in which rain occurred and precipitation rates lower than 0.1 mm h^{-1} were excluded from the calculation (Dai *et al.*, 1999). The precipitation intensity was defined as the accumulated rainfall amount during each hour in which precipitation occurred (units: mm h^{-1}). Following Yu *et al.* (2007a) and Chen *et al.* (2009), the duration of a rainfall event was defined as the number of hours from the beginning to the end of a rainfall event, and the corresponding intermittence should be no longer than 1 h. Thus, those rainfall events with intermittences greater than 1 h were regarded as two different rainfall events.

Generally, precipitation decreases from more than 1800 mm $year^{-1}$ in southeastern coastal areas to less than 50 mm $year^{-1}$ in northwestern inlands (Qian and Lin,

2005). Thus, a fixed threshold to define the precipitation categories from light to heavy may not be appropriate for all regions. To scientifically reflect regional climate features, the percentile thresholds were adopted to define different categories. Percentiles near 100% represent very heavy precipitation, whereas those percentiles near zero signify very light precipitation (Frich *et al.*, 2002; Zhang and Zhai, 2011; Huang and Wen, 2013). It is notable that although the absolute value is variable from site to site, for a station, the class intervals are fixed based on the quantiles of the entire sample.

Following Bonsal *et al.* (2001) and Zhai and Pan (2003), hourly precipitation was first ranked in an ascending order $x_1, x_2, \ldots, x_m, \ldots, x_n$. The probability ($P$) that a random value is less than or equal to the rank of the value x_m was calculated as $P=(m-0.31)/(n+0.38)$, where m is the sequence number of x_m, and n is the total frequency of a station. Based on the above-mentioned method, a total of ten precipitation categories were defined as the percentiles of 20, 30, …, 90, 95 and 100%, where 20% indicates the range from the minimum precipitation value up to the 20th percentile, 30% denotes the precipitation category between 20 and 30%, and so on. As the minimum recording value is 0.1 mm h^{-1}, the frequency of 0.1 mm h^{-1} was too high to distinguish the main precipitation intensity, so the lowest category was defined as 20%. Figure 2(b) shows the 95th percentile, i.e. the extreme heavy precipitation category during the warm season of 1982–2012 at each station. The values ranged from more than 16 mm h^{-1} in southeast coastal areas to only 3 mm h^{-1} in the northwest part of the study region, with an additional region of relatively strong precipitation located in the Sichuan Basin in southwest China.

Referring to Karl and Knight (1998), it is possible to estimate the proportion of any trend in the total precipitation amount that can be attributed to the changes in the precipitation frequency versus the changes in the precipitation intensity. The trend caused by the rainfall frequency changes was therefore defined as

$$b_e = \overline{P_e}\left(b_f\right) \tag{2}$$

where $\overline{P_e}$ is the average precipitation amount per class interval (mm h^{-1}) and b_f is the trend of any specific class intervals (h year^{-1}), so b_e is expressed in mm year^{-1} or the proportion (%) of mean precipitation. The trend related to the intensity component was calculated by

$$b_i = b - b_e \tag{3}$$

where b is the trend of total precipitation in any category (mm year^{-1}). To compare results in different regions, the trends were expressed as a percentage of the mean precipitation over a region.

Additionally, because precipitation amount is determined by frequency and intensity, the frequency can also be divided into two separate parts: the number of rainfall events and the duration hours of each event. Following Equations (2) and (3), the contributions of rainfall events were divided into the number and duration of precipitation events. The contribution of precipitation events (E_e) was calculated by

$$E_e = \overline{D_e} \bullet E_f \tag{4}$$

where $\overline{D_e}$ is the average duration of precipitation events and E_f is the overall trend of precipitation events (events year^{-1}). The trend related to the duration component E_i was calculated by

$$E_i = E - E_e \tag{5}$$

where E is the trend of precipitation frequency in a region (h year^{-1}).

A linear trend was calculated by using the time series of the precipitation in different categories. The linear function of time t can be written as

$$X = A + Bt \tag{6}$$

where X is the precipitation amount or frequency, B represents the regression coefficient calculated using the least-squares method and A denotes the intercept. Subsequently, the relative trend was given by $b = 10\,B/X_p$, where X_p is the average value of a typical precipitation region during 1982–2012. The Student's t-test and 'field significance' resampling approach (Livezey and Chen, 1983; Westra *et al.*, 2013) were used in this study to verify the significant level.

To investigate and compare the quantitative trends of a meteorological element, the climatic trend coefficient (Shi *et al.*, 2006) was also utilized.

$$r_{xt} = \frac{\sum_{t=1}^{n}\left(x_t-\bar{x}\right)\left(t-\frac{n+1}{2}\right)}{\sqrt{\sum_{t=1}^{n}\left(x_t-\bar{x}\right)\left(t-\frac{n+1}{2}\right)^2}} \tag{7}$$

where r_{xt} is defined as the correlation coefficient between an element's series and the sequence of natural numbers of 1, 2, 3, … n, and can be tested by means of the Student's t-test method. As r_{xt} is a unitless quantity, its magnitudes can be compared and utilized to estimate the intensity of secular trends for different elements. It is applicable to the investigation on the spatial features of a large-scale meteorological field.

3. Geographic distribution of precipitation features

To improve our understanding of the changing characteristics of precipitation, we first calculated the climatological mean and variation coefficient using the hourly precipitation data set. Figure 3(a) and (c) show the mean rainfall amount and frequency distribution during the warm season, respectively. The rainfall amount decreased from more than 1600 mm in southeastern coastal areas to less than 200 mm in northwestern inland areas. A large gradient zone around 600 mm can be detected near 32–34°N, which generally acts as the climatological boundary line between the north and south parts of eastern China (Zhang

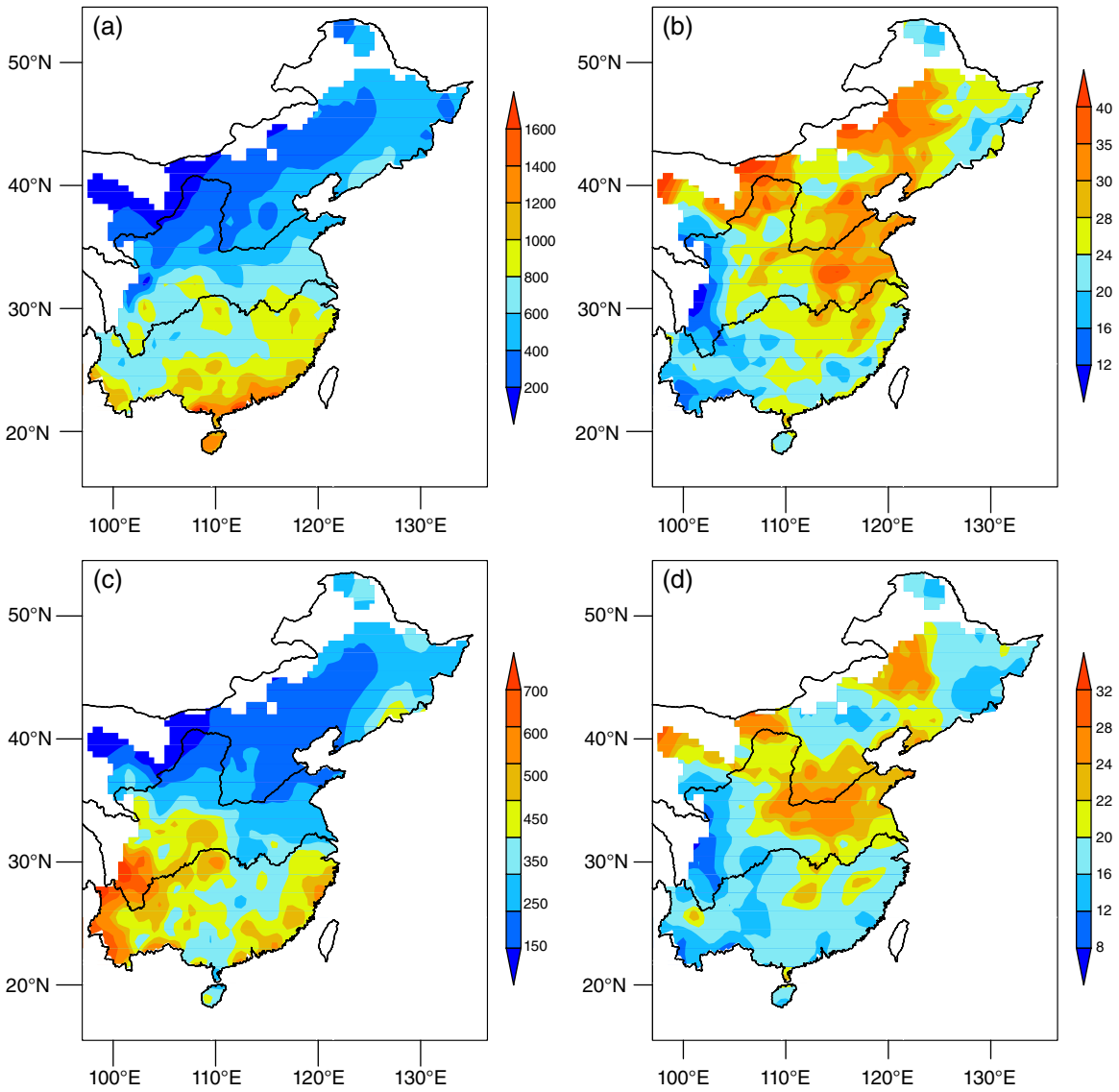

Figure 3. Mean precipitation (a, units: mm) and variation coefficient of precipitation (b, units: %); mean frequency (c, units: h) and variation coefficient of frequency (d units: %) during warm season for 1982–2012.

and Zhang, 1979; Zhang *et al.*, 2012). In contrast to rainfall amount, the distribution of the rainfall frequency featured two key areas of high rainfall frequency, which were located in the southwestern and southeast coastal areas of China. The former may have been related to the topography of the region, such as the Tibetan Plateau and Yunnan-Guizhou Plateau (Yu *et al.*, 2004), and the latter may have occurred as a result of the ample moisture conditions in the coastal region.

The variation coefficient (C_v), expressed as a percentage, was calculated using $C_v = S/M \times 100\%$, where the standard deviation and the mean value are denoted by S and M, respectively. Thus, C_v denotes a relative variation of the standard deviation. The variation coefficients of precipitation and frequency are shown in Figure 3(b) and (d). The higher C_v regions were found in northern China, mainly including the upper and lower reaches of the Huanghe River and northeast China. Lower C_v regions were mainly observed in the eastern Tibetan Plateau and south of the Yangtze River. The centres of larger C_v in northern China are usually affected by severe drought, for example, those located mainly along the Huanghe River valley (Wang *et al.*, 2011; Li *et al*, 2014), where the C_v is more than 30% in Figure 3(b) and above 24% in Figure 3(d).

As shown in Figure 4(a), the average precipitation intensity decreased from southeast to northwest with a maximum of 4.13 mm h^{-1} and a minimum of 0.72 mm h^{-1}, and a relative higher value was also found in the Sichuan Basin in southwest China. The distribution pattern of average precipitation intensity is very similar to the 95th percentile of the hourly precipitation (Figure 2(b)). As the climate average value cannot reflect the extreme value of the maximum precipitation intensity, Figure 4(b) shows the mean frequency of precipitation intensity greater than 20 mm h^{-1} from May to September during 1982–2012. In the past 31 years, the highest frequency of extreme intensity mainly located in coastal areas of South China, and the general high frequency is in Huang-Huai River

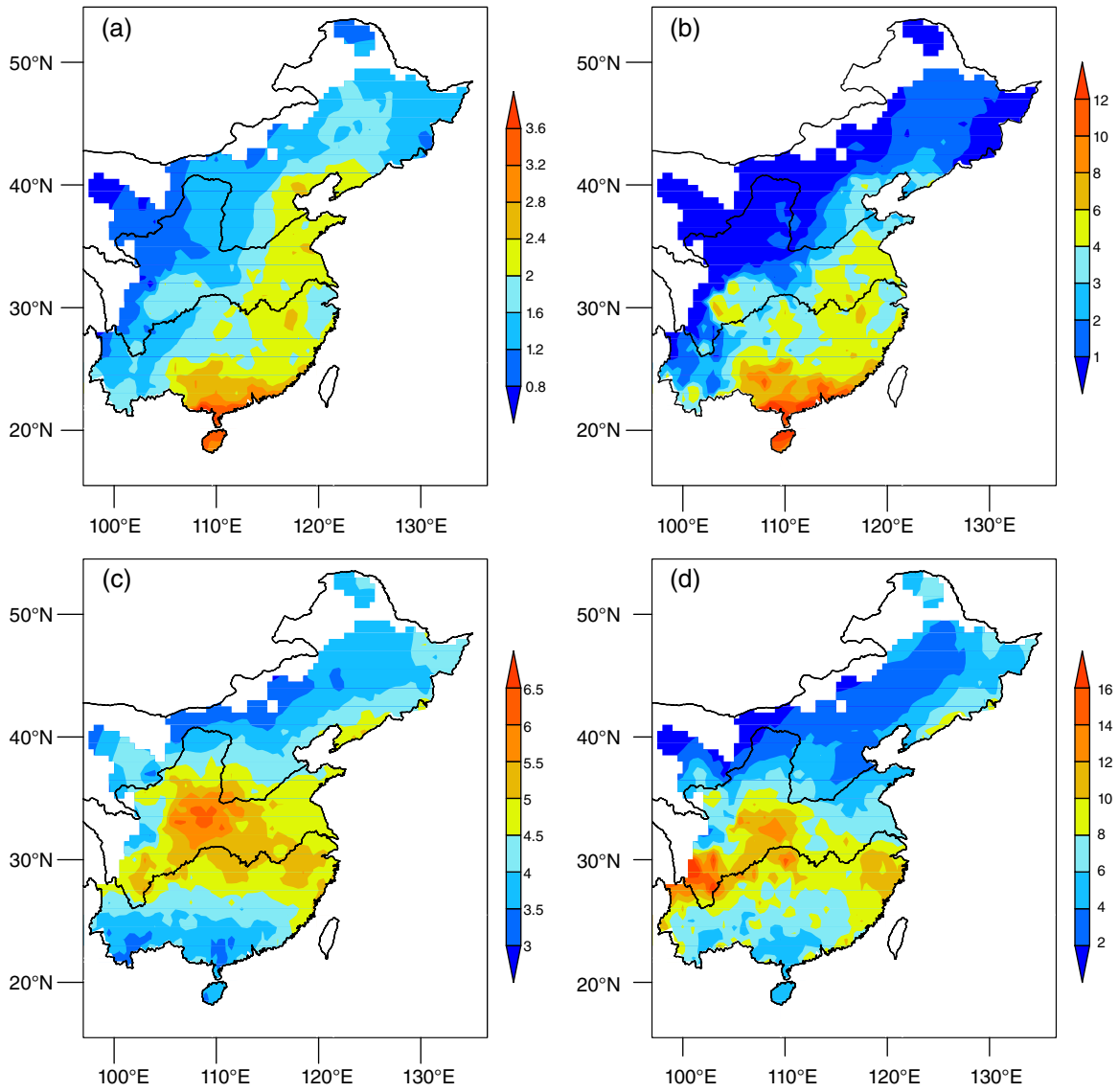

Figure 4. Mean precipitation intensity (a, units: mm h^{-1}) and mean frequency (expressed by number of hours) of precipitation intensity greater than 20 mm h^{-1} (b, units: h), and mean duration of rainfall events (c, units: h) and average frequency of rainfall events longer than 12 h (d) in 1982–2012.

Basin, the middle and lower reaches of the Yangtze River and the Sichuan Basin.

The mean duration of rainfall events is revealed in Figure 4(c). It shows a significant 'sandwich-like pattern' with higher values located in central China, specifically around the Yangtze River and Huanghe River, whereas relatively low values were distributed in southern and northern China. It is very interesting to note that the highest values were located in western China along the Qinling Mountains, with an average duration of about 6 h per rainfall event. The long-duration rainfall events mainly occurred in September, referred to as the 'Autumn rainfall over western China' (Gao and Guo, 1958; Bai and Dong, 2004). The long-duration rainfall events located along the Yangtze River and the coastal areas may be related to the Mei-yu front (Ding, 1992; Sun *et al.*, 2010) and tropical cyclones (Wang *et al.*, 2008; Zhang *et al.*, 2009), respectively. The high frequencies of rainfall events longer than 12 h (Figure 4(d)) are found in southeast coastal areas, western China along the Qinling Mountains and southwest China. In addition, the longest duration on record is about 125 h in southeast coastal areas of China in June, 2002 (not shown).

4. Regional trends in precipitation characteristics

4.1. Regional divisions

In Section 3, it was shown that the characteristics of precipitation are different from region to region. Therefore, the detailed precipitation trend should be evaluated on a regional basis. In previous studies, the regionalization of climate was usually performed based on administrative boundaries, watersheds or topography (Zhao *et al.*, 2012; Zhang and Cong, 2014). Such boundaries may suffer from subjectivity, due to a lack of consideration of the inner linkages among meteorological stations and studied areas. Therefore, the rotated empirical orthogonal

Table 1. Percentage of the total normalized variance explained by each of the first 10 initial and final (rotated) principal components.

Component number	Variance explained (%)	
	Principal component	Rotated principal component
1	13.73	8.54
2	8.70	6.87
3	7.67	7.40
4	6.94	7.84
5	5.92	7.42
6	5.07	5.98
7	4.64	5.40
8	4.03	5.14
9	3.89	5.10
10	2.94	3.83
Total	63.52	63.52

function (REOF) analysis was applied to detect the similar localized modes of the hourly precipitation objectively (Horel, 1981). According to varimax REOF analysis (Kaiser, 1958), eigenvalue separations were used to test the number of regions, and the maximum loading (where $\gamma = 0.5$ or $\gamma = -0.5$), was used to determine the climate divisions. Nine spatial patterns were determined over central eastern China. The variance contribution of the first nine EOF/REOF vectors, whose accumulated variance contribution exceeded 60%, is shown in Table 1.

According to the locations of the high loading values, central eastern China can be divided into nine regions as shown in Figure 5: Northeast China (NE), Bohai-sea Rim (BR), the Huang-Huai River Basin (HH), the Loess Plateau (LP), the middle reaches of the Yangtze River Basin (MYR), the lower reaches of the Yangtze River Basin (LYR), south China (S), southeast coastal areas (SE) and Yunnan district (YN). Compared with factors such as terrain and rivers, these nine regions can reasonably represent the geographic features in Figures 3 and 4, and thus

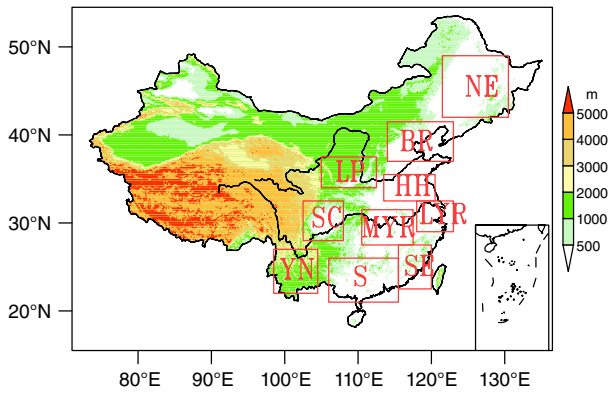

Figure 5. Schematic diagram of the ten sub-regions over central eastern China, and these regions are: Northeast China (NE), Bohai-sea Rim (BR), Huang-Huai River Basin (HH), Loess Plateau (LP), Middle reaches of Yangtze River Basin (MYR), Lower reaches of Yangtze River Basin (LYR), South China (S), South-East coastal areas (SE) and Yunnan district (YN). The shading colors denote altitude (units: m).

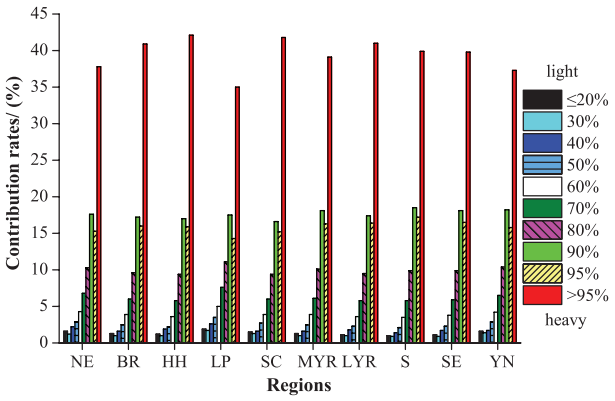

Figure 6. The contribution rate of different categories in total precipitation.

the division of results based on the hourly precipitation was deemed appropriate. The Sichuan Basin (SC), located in the east of the Tibetan Plateau, features heavier precipitation more often than other regions at the same longitude (Figure 3), with peaks from the night to early morning (Yu *et al.*, 2007b; Qian *et al.*, 2015). Hence the Sichuan Basin was added as a typical region for analysis.

The proportion of different precipitation categories in the total precipitation is shown in Figure 6. Extreme rainfall had the highest contribution, although it only accounted for about 5% of the total frequency. In addition, the upper 10% of hourly precipitation events constituted about 49–58% of the total rainfall amount in central eastern China. This shows that the heavy rainfall was concentrated in time and therefore it is necessary to describe changes in different intensity categories.

4.2. Regional trends in precipitation amount and frequency across different categories

Figure 7(a) shows the linear trends of precipitation amount in different categories, where the abscissa indicates the level of precipitation intensity from light to heavy, and the ordinate indicates the linear trend of each category. A common feature can be found that the upper decile contributed more strongly to the precipitation changes, whereas the contributions of the moderate to light precipitation were relatively smaller. The heavy rainfall events in the top decile dominated the changes in the total precipitation amount over central eastern China.

However, regional differences were also apparent. For S and SE, the precipitation amount changes passed the significance test of $\alpha = 0.1$, and the positive trend was much more obvious in the extreme heavy precipitation category, with trend values of 3.01 and 4.07% per decade, respectively. In S, all levels of precipitation featured increasing trends, but in SE, there were weak downward trends in the light precipitation category, whereas gradually increasing trends were detected in the moderate to extreme heavy precipitation category. In NE and SC, precipitation declined in all categories, and there were significant decreasing trends at the intensity levels of 30–40% and 40–50% in NE, and below 30% in SC. These results revealed

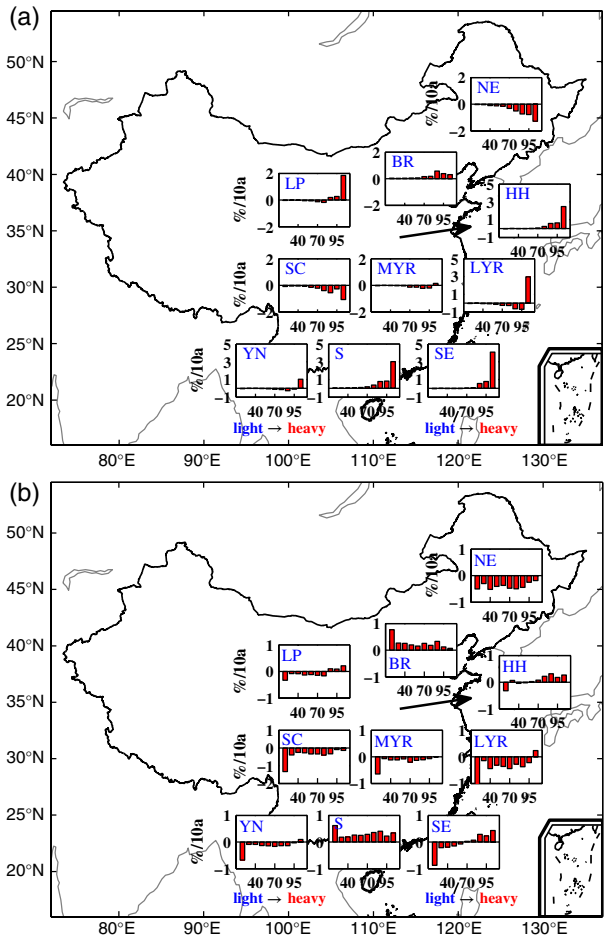

Figure 7. Trends of precipitation amount (a) and precipitation frequency (b) at different categories. Trends are expressed as a percentage of the mean precipitation amount and frequency per decade. Value plotted at 20th percentile represents the trend from the lowest percentile to the 20th percentile, and value plotted for the 30th percentile represents the trend for the 20th to the 30th percentile. Value plotted at the 95th percentile represents the trend for the 95th to the highest percentiles.

that light precipitation decreased more significantly than heavy precipitation in these two areas, but the greatest contribution to precipitation belonged to the extreme heavy rainfall category, with downward trends of −1.28 and −1.06% per decade, separately. In other regions, such as BR, LP and HH, increasing trends were significant in the heavy and moderate precipitation categories, whereas in MYR and YN the negative trends were very weak. For LYR, an increasing trend in extreme heavy precipitation was detected.

Changes in precipitation can be caused by both frequency variations and intensity changes. As shown in Figure 7(b), precipitation frequency changes were mainly reflected in the lower decile of intensity categories. In terms of regional distribution, rainfall frequency was characterized by a decreasing trend in each category in NE and SC. Significant decreasing trends at the 90% confidence level were detected in the categories of 30–40% and 40–50% in NE, and below 30% in SC. In S and BR, the precipitation frequency increased, and this was mainly reflected in the increase in light precipitation in BR, whereas for S, the increasing trends were found in the categories from light to heavy precipitation, and the trend of extreme precipitation was significant at the 95% confidence level. For HH, light precipitation featured a decreasing trend, but moderate and heavy rainfall categories behaved in the opposite manner. In LP and SE, the frequency of light precipitation decreased, whereas moderate and heavy precipitation featured increasing trends. For MYR, LYR and YN, the total frequency decreased, but the frequency of extreme heavy precipitation exhibited an increasing trend, which implies that the precipitation shifted from weak intensity to strong intensity. Besides the Student's *t*-test, a field significance resampling-based procedure (Livezey and Chen, 1983; Westra *et al.*, 2013) was also used, but the results showed that only 15 trends to be significant. This may caused by the stations, with increasing and decreasing, precipitation appear to be randomly distributed over the studied area and it is difficult to isolate a clear geographic pattern, as mentioned by Min *et al.* (2011), Westra *et al.* (2013) and Wang *et al.* (2013).

It is interesting to compare Figure 7(a) and (b). For the same region, the general trend was similar in precipitation amount and frequency. However, although frequency changed more obviously in the light rainfall category, heavy rainfall contributed more strongly to the total precipitation amount. This was due to the low intensity of light rainfall, so the accumulated precipitation amount was not as high as heavy precipitation.

Moreover, we defined three major rain types: light rain (LR) which below the 30th percentile, moderate rain (MR) which between 40th and 70th percentile and extreme heavy rain (EHR) which above the 95th percentile. The trends of frequency were showed in Figure 8, and positive changes dominate most of the EHR, while negative trends were detected on LR and MR in most sub-regions. In average of the ten sub-regions over central, the EHR showed a significant increasing trend (90% confidence level) of

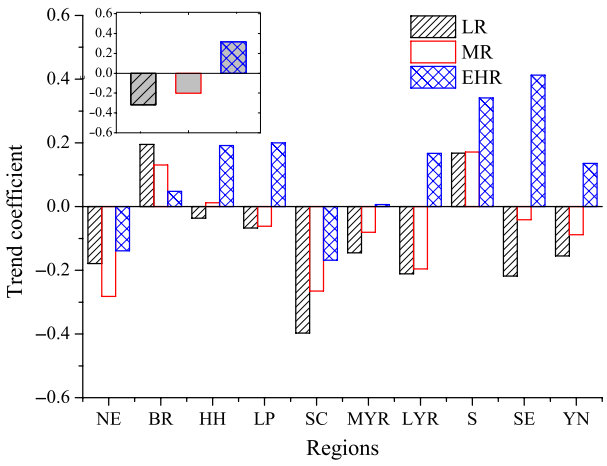

Figure 8. The climatic trend coefficients of light rain (LR), moderate rain (MR) and extreme heavy rain (EHR) in ten sub-regions and the average value (bar chart in the upper left), and the *t*-test method is used to detect whether the trend of a series reaches statistical significance.

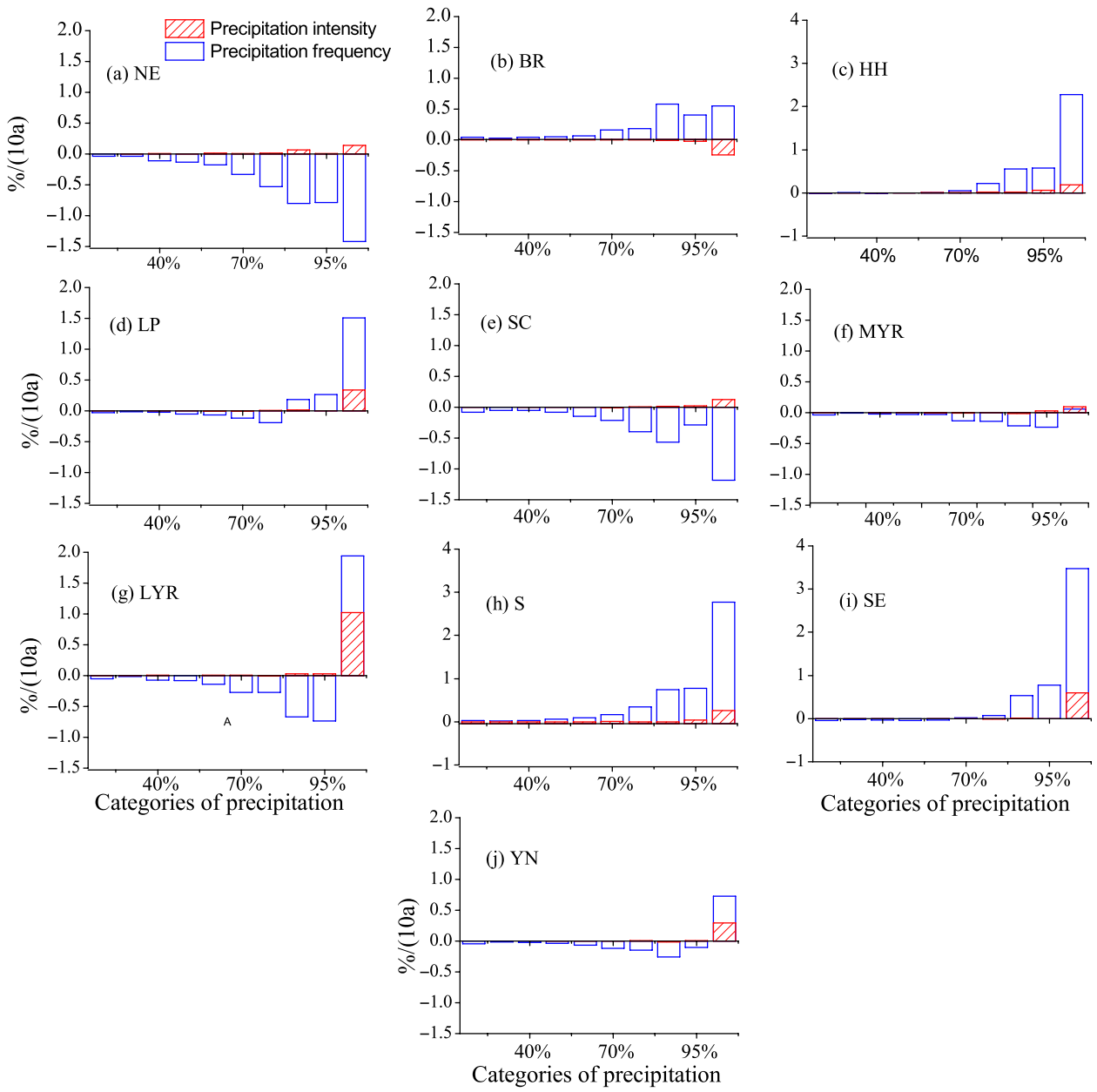

Figure 9. The trends of frequency and intensity to precipitation amount changes at different category for ten sub-regions. Contributions are expressed as a percentage of the mean precipitation amount per decade and the bar chart stands for the same meaning as in Figure 7.

5.12 h decade^{-1}, and the LR showed a significant decreasing trend (90% confidence level) of 22.45 h decade^{-1} over central eastern China (not shown), i.e. there is a shift from light precipitation towards heavy precipitation. These trends are consistent with the pattern of 'increasing in extremely heavy rainfall at the expense of light rainfall' mentioned by Rajah *et al.* (2014).

4.3. The contribution of frequency and intensity to total precipitation changes

As mentioned above, the overall trends in precipitation amount resulted from changes in both frequency and intensity of precipitation. Using Equations (2) and (3), the contributions of precipitation frequency and intensity were calculated and the results are shown in Figure 9. In comparison to precipitation intensity, changes in rainfall frequency, especially the frequency of the top decile, provided greater contributions to the total precipitation changes than other deciles. However, for the heavy rainfall category, intensity changes were also very important.

In the regions where precipitation amount increased significantly, i.e. S and SE, the trends were mainly due to increases in heavy and extreme heavy rainfall frequency, although the rainfall intensity also showed an increasing trend. In NE and SC, where precipitation showed clear negative trends in every category, the changes were mainly due to the decline in frequency, whereas the precipitation intensity did not change significantly (although the intensity of extreme heavy precipitation showed positive trends). For regions with no significant trend, both

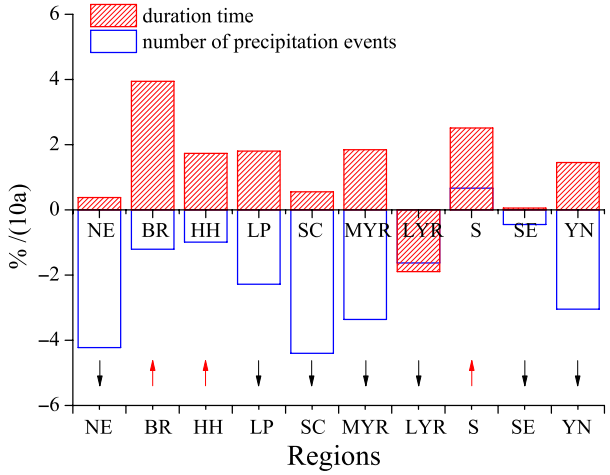

Figure 10. Contribution of the number and the duration of precipitation events to the total frequency changes. The upward (downward) arrow indicates the positive (negative) trend of total precipitation frequency in this region.

frequency and intensity showed rising trends in extreme heavy rainfall in HH, LP, MYR, LYR and YN. In BR, meanwhile, the intensity of heavy precipitation decreased while the frequency showed increasing trends. This is also an indirect proof of the diversity and complexity of the key factors that influence regional precipitation changes in China.

In general, the change in precipitation frequency was the main reason for the variance of precipitation amount over central eastern China and the contribution rate was more than 95%. In some categories, the changes in rainfall frequency and intensity were opposite, but the trend of precipitation intensity was lower than that of rainfall frequency. Overall, the trends of precipitation were determined by the frequency changes.

4.4. The contribution of rainfall events and its duration in frequency changes

For the data limitations of daily data, previous studies lacked the ability to accurately determine the precipitation duration at hourly intervals (Trenberth *et al.*, 2003), so it is necessary to use the hourly data to analyse the changes of precipitation duration. Precipitation frequency is the total accumulated hours in which precipitation occurred, and it is also the sum of the duration of every rainfall event. Using the same method as precipitation amount is determined by frequency and intensity, the frequency can also be divided into the number of rainfall events and the duration hours of every event, and calculated by Equations (4) and (5).

Figure 10 depicts the relative contributions of precipitation events and duration time to the changes of frequency. The upward (downward) arrow indicates a positive (negative) trend of total precipitation frequency in the region. It shows that the area-averaged rainfall duration (number of precipitation events) increased (decreased) in all regions except LYR. In different regions, such as S, the increase in duration time produced a larger contribution to the total frequency trends, accounting for 79.1% of the total change. However, in the areas with decreasing trends in every category (NE, SC), a sharp decline was found in the number of precipitation events, with a contribution rate of 110.0 and 114.3%, respectively. The rates larger than 100% occurred as a result of the precipitation events and their durations acting opposite to each other, but the changes to the precipitation events were on balance more important.

Therefore, the increased rainfall hours were largely caused by the prolonged rainfall events, whereas the decreased rainfall hours were mainly due to reduction in the number of rainfall events rather than reduced duration of each event. To some degree, the number of precipitation events reflected the frequency of the rainfall process, and the duration denoted the intensity of the precipitation process. This implies that the precipitation frequency over central eastern China has a potential trend for less frequent rainfall events that are much longer in duration, just as in the proverb 'it never rains but it pours' (Trenberth, 1998; Trenberth, 2011). This result is consistent with the research of Yu *et al.* (2010), which showed that the mean rainfall hours have increased because of the prolonged rainfall duration in the mid-lower reaches of the Yangtze River based on hourly data. A positive trend in the maximum number of consecutive wet days was detected in southeast China except near the coast, and a negative trend was found along the Huanghe River valley based on daily data (Qian and Lin, 2005; Zhang *et al.*, 2011a). While the enhanced number of consecutive dry days in east China (Qian and Lin, 2005; Alexander *et al.*, 2006; Wang and Fu, 2013) is connected to the decreases of light and moderate precipitation. Over Europe, Zolina *et al.* (2010) found that the duration of rainfall events has become longer since short-rain events have been regrouped into prolonged wet spells from 1950 to 2008. Perhaps the longer duration of precipitation events are related to the slower progression of planetary waves in 500-hPa height fields, thus storms were expected to propagate more slowly resulting in more persistent weather patterns (Francis and Vavrus, 2012; Screen and Simmonds, 2014; Guilbert *et al.*, 2015). Further investigations will be needed to explain the mechanisms about these changes in China.

5. Conclusions

On the basis of an intensive hourly precipitation data set, the precipitation features and regional trends in both rainfall amount and frequency were investigated over central eastern China during the warm season from 1982 to 2012. The contributions of frequency and intensity to the precipitation changes were subsequently compared for different precipitation intensity categories. In addition, the precipitation frequency was evaluated by the number of rainfall events and the duration of each event. The main findings of this study are summarized as follows:

1. The spatial features of precipitation were significant during the warm season and the mean precipitation amount and intensity decreased from southeastern

coastal areas to northwestern inland areas. In contrast, the precipitation duration showed a remarkable 'sandwich-like structure', with a higher value located in central China and relatively lower values distributed in southern and northern China. A higher variation coefficient of precipitation amount and frequency was found in northern China, such as along the Huanghe River valley.

2. Generally, the extreme heavy rainfall showed a significant increasing trend while the light rainfall showed a significant decreasing trend over central eastern China, which is consistent with the pattern of 'it never rains but it pours'. According to the EOF/REOF vectors, a total of 10 spatial patterns were determined over central eastern China. In south and southeast China, significantly increasing trends were found, whereas in Bohai-sea Rim and the Sichuan Basin, precipitation amounts showed a declining trend in each precipitation category.
3. The changes in precipitation frequency, especially the frequency of heavy and extreme heavy rainfall, were the main reason for the variation of precipitation amount over central eastern China, and the contribution rate of frequency changes was greater than 95%. Therefore, the trend of precipitation was mainly caused by frequency changes, but to the heavy rainfall category, intensity changes were also very important.
4. Meanwhile, the increased precipitation frequency was largely caused by the prolonged duration of rainfall events, but the decreased rainfall hours were mainly due to the reduction in the number of rainfall events. The area-averaged rainfall duration (number of precipitation events) increased (decreased) in all regions except for the lower reaches of the Yangtze River, which implies that the precipitation frequency over central eastern China has a potential trend for much longer and less-frequent rainfall events.

Precipitation processes are affected by many factors, such as the East Asian summer monsoon, the Indian monsoon, the El Niño–Southern Oscillation and Pacific Decadal Oscillation, atmospheric aerosols, surface air (or sea) temperature, changes in precipitable water vapour, precipitation efficiency, dynamical contributions and the microphysics of cloud droplets. These reasons possibly lead to complexity of precipitation changes. As regional precipitation variability is one of the major features of China's climatology, our results suggest that the response of precipitation characteristics may vary among different regions over central eastern China, and that perhaps local and mesoscale features are also important. Siler and Roe (2014) evaluated the response of orographic precipitation to surface warming, and recently Shi and Durran (2015) found the increases are larger on the climatological leeward side than on the windward side of a midlatitude mountain based on idealized simulations. Groisman *et al.* (2012) suggested that the changing crop patterns and water use over large areas may feed back to the water cycle and result in changes of atmospheric water vapour and the precipitation recycling ratio. Therefore, further work is needed to study the role of local or mesoscale factors on precipitation changes through models or empirical analysis.

Acknowledgements

The precipitation data were provided by the National Meteorological Information Centre of the China Meteorological Administration (CMA). This research was supported by the CMA (Grant No. GYHY201406002), the Key Program of the Chinese Academy of Sciences (Grant No. 2012CB417201) and the National Natural Science Foundation of China (Grant No. 41205027). The authors would like to thank the two revivers who provided constructive criticism and suggestions that greatly improved the paper.

References

Alexander LV, Zhang X, Peterson TC, Caesar J, Gleason B, Klein Tank AMG, Haylock M, Collins D, Trewin B, Rahimzadeh F, Tagipour A, Ambenje P, Rupa Kumar K, Revadekar JV, Griffiths G, Vincent L, Stephenson D, Burn J, Aguilar E, Brunet M, Taylor M, New M, Zhai P, Rusticucci M, Vazquez-Aguirre JL. 2006. Global observed changes in daily climate extremes of temperature and precipitation. *J. Geophys. Res.* **111**: D05109, doi: 10.1029/2005JD006290.

Allan RP, Soden BJ, John VO, Ingram W, Good P. 2010. Current changes in tropical precipitation. *Environ. Res. Lett.* **5**: 025205, doi: 10.1088/1748-9326/5/2/025205.

Asadieh B, Krakauer NY. 2015. Global trends in extreme precipitation: climate models versus observations. *Hydrol. Earth Syst. Sci.* **19**(2): 877–891.

Bai H, Dong W. 2004. Climate features and formation causes of Autumn rain over Southwest China. *Plateau Meteorol.* **23**(6): 884–889 (in Chinese).

Beck F, Bárdossy A, Seidel J, Müller T, Sanchis E, Hauser A. 2015. Statistical analysis of sub-daily precipitation extremes in Singapore. *J. Hydrol.* **3**: 337–358.

Berg P, Haerter JO. 2013. Unexpected increase in precipitation intensity with temperature – a result of mixing precipitation types? *Atmos. Res.* **119**: 56–61.

Berg P, Haerter JO, Thejll P, Piani C, Hagemann S, Christensen JH. 2009. Seasonal characteristics of the relationship between daily precipitation intensity and surface temperature. *J. Geophys. Res.* **114**: D18102, doi: 10.1029/2009JD0120 08.

Berg P, Moseley C, Haerter JO. 2013. Strong increase in convective precipitation in response to higher temperatures. *Nat. Geosci.* **6**: 181–185.

Bonsal BR, Zhang X, Vincent LA, Hong WD. 2001. Characteristics of daily and extreme temperatures over Canada. *J. Clim.* **14**(9): 1959–1976.

Chen H, Zhou T, Yu R, Li J. 2009. Summer rain fall duration and its diurnal cycle over the US Great Plains. *Int. J. Climatol.* **29**(10): 1515–1519.

Dai A, Giorgi F, Trenberth KE. 1999. Observed and model-simulated diurnal cycles of precipitation over the contiguous United States. *J. Geophys. Res.* **104**(D6): 6377–6402, doi: 10.1029/98jd02720.

Ding Y. 1992. Summer monsoon rainfalls in China. *J. Meteorol. Soc. Jpn.* **70**(1B): 373–396.

Donat MG, Alexander LV, Yang H, Durre I, Caesar R. 2013. Global land-based datasets for monitoring climatic extremes. *Bull. Am. Meteorol. Soc.* **94**(7): 997–1006.

Dunn RJH, Willett KM, Thorne PW, Woolley EV, Durre I, Dai A, Parker DE, Vose RS. 2012. HadISD: a quality-controlled global synoptic report database for selected variables at long-term stations from 1973–2011. *Clim. Past* **8**: 1649–1679.

Francis JA, Vavrus SJ. 2012. Evidence linking Arctic amplification to extreme weather in mid-latitudes. *Geophys. Res. Lett.* **39**: L06801, doi: 10.1029/2012GL05 1000.

Frich P, Alexander LV, Della-Marta P, Gleason B, Haylock M, Klein Tank AM, Peterson T. 2002. Observed coherent changes in climatic extremes during the second half of the twentieth century. *Clim. Res.* **19**(3): 193–212.

Fujibe F, Yamazaki N, Katsuyama M, Kobayashi K. 2005. The increasing trend of intense precipitation in Japan based on four-hourly data for a hundred years. *SOLA* **1**: 41–44.

Gao Y, Guo Q. 1958. On the Autumn raining area in China. *Acta Meteorol. Sin.* **29**(4): 264–273 (in Chinese).

Groisman PY, Knight RW, Easterling DR, Karl TR, Hegerl GC, Razuvaev VN. 2005. Trends in intense precipitation in the climate record. *J. Clim.* **18**(9): 1326–1350.

Groisman PY, Knight RW, Karl TR. 2012. Changes in intense precipitation over the central United States. *J. Hydrometeorol.* **13**(1): 47–66.

Guilbert J, Betts AK, Rizzo DM, Beckage B, Bomblies A. 2015. Characterization of increased persistence and intensity of precipitation in the northeastern United States. *Geophys. Res. Lett.* **42**(6): 1888–1893.

Haerter JO, Berg P. 2009. Unexpected rise in extreme precipitation caused by a shift in rain type? *Nat. Geosci.* **2**: 372–373.

Haerter JO, Berg P, Hagemann S. 2010. Heavy rain intensity distributions on varying time scales and at different temperatures. *J. Geophys. Res.* **115**: D17102, doi: 10.1029/2009JD013384.

Hardwick-Jones R, Westra S, Sharma A. 2010. Observed relationships between extreme sub-daily precipitation, surface temperature, and relative humidity. *Geophys. Res. Lett.* **37**: L22805, doi: 10.1029/2010GL045081.

Horel JD. 1981. A rotated principal component analysis of the interannual variability of the Northern Hemisphere 500 mb height field. *Mon. Weather Rev.* **109**(10): 2080–2092.

Huang G, Wen G. 2013. Spatial and temporal variations of light rain events over China and the mid-high latitudes of the Northern Hemisphere. *Chin. Sci. Bull.* **58**(12): 1402–1411.

Kaiser HF. 1958. The varimax criterion for analytic rotation in factor analysis. *Psychometrika* **23**(3): 187–200.

Karl TR, Knight RW. 1998. Secular trends of precipitation amount, frequency, and intensity in the United States. *Bull. Am. Meteorol. Soc.* **79**(2): 231–241.

Kiktev D, Sexton D, Alexander L, Folland C. 2003. Comparison of modeled and observed trends in indices of daily climate extremes. *J. Clim.* **16**(22): 3560–3571.

Kunkel KE, Easterling DR, Redmond K, Hubbard K. 2003. Temporal variations of extreme precipitation events in the United States: 1895–2000. *Geophys. Res. Lett.* **30**(17): 1900, doi: 10.1029/2003gl018052.

Lau WKM, Wu HT, Kim KM. 2013. A canonical response of precipitation characteristics to Global Warming from CMIP5 models. *Geophys. Res. Lett.* **40**: 3163–3169, doi: 10.1002/grl.50420.

Lenderink G, Van Meijgaard E. 2008. Increase in hourly precipitation extremes beyond expectations from temperature changes. *Nat. Geosci.* **1**(8): 511–514.

Li J, Yu R, Yuan W, Chen H. 2011. Changes in duration related characteristics of late-summer precipitation over eastern China in the past 40 years. *J. Clim.* **24**(21): 5683–5690.

Li Y, Wang J, Li Y, Wang S, Sha S. 2014. Study of the sustainability of drought in China. *J. Glaciol. Geocryol.* **36**(5): 1131–1142 (in Chinese).

Liu B, Xu M, Henderson M, Qi Y. 2005. Observed trends of precipitation amount, frequency, and intensity in China, 1960–2000. *J. Geophys. Res.* **113**: D08103, doi: 10.1029/200 4jd004864.

Livezey R, Chen W. 1983. Statistical field significance and its determination by Monte Carlo techniques. *Mon. Weather Rev.* **111**(1): 46–59.

Min SK, Zhang X, Zwiers FW, Hegerl GC. 2011. Human contribution to more-intense precipitation extremes. *Nature* **470**(7334): 378–381.

Molnar P, Fatichi S, Gaál L, Szolgay J, Burlando P. 2015. Storm type effects on super Clausius–Clapeyron scaling of intense rainstorm properties with air temperature. *Hydrol. Earth Syst. Sci.* **19**(4): 1753–1766.

O'Gorman PA. 2015. Precipitation extremes under climate change. *Curr. Clim. Change Rep.* **1**(2): 49–59.

Qian W, Lin X. 2005. Regional trends in recent precipitation indices in China. *Meteorol. Atmos. Phys.* **90**(3–4): 193–207.

Qian W, Fu J, Yan Z. 2007. Decrease of light rain events in summer associated with a warming environment in China during 1961–2005. *Geophys. Res. Lett.* **34**(11): L11705, doi: 10.1029/2007gl029631.

Qian T, Zhao P, Zhang F, Bao X. 2015. Rainy-season precipitation over the Sichuan Basin and adjacent regions in Southwestern China. *Mon. Weather Rev.* **143**(1): 383–394.

Rajah K, O'Leary T, Turner A, Petrakis G, Leonard M, Westra S. 2014. Changes to the temporal distribution of daily precipitation. *Geophys. Res. Lett.* **41**(24): 8887–8894.

Screen JA, Simmonds I. 2014. Amplified mid-latitude planetary waves favour particular regional weather extremes. *Nat. Clim. Change* **4**: 704–709, doi: 10.1038/NCLIMATE2271.

Sen Roy S. 2009. A spatial analysis of extreme hourly precipitation patterns in India. *Int. J. Climatol.* **29**(3): 345–355.

Shi X, Durran DR. 2015. Estimating the response of extreme precipitation over mid-latitude mountains to global warming. *J. Clim.* **28**(10): 4246–4262.

Shi N, Yi Y, Gu J, Xia D. 2006. On the correlation of nonlinear variables containing secular trend variations: numerical experiments. *Chin. Phys.* **15**(9): 2180–2184.

Siler N, Roe G. 2014. How will orographic precipitation respond to surface warming? An idealized thermodynamic perspective. *Geophys. Res. Lett.* **41**(7): 2606–2613.

Sillmann J, Kharin VV, Zhang X, Zwiers F, Bronaugh D. 2013. Climate extremes indices in the CMIP5 multimodel ensemble: Part 1. Model evaluation in the present climate. *J. Geophys. Res.* **118**(4): 1716–1733.

Sun J, Zhao S, Xu G, Meng Q. 2010. Study on a mesoscale convective vortex causing heavy rainfall during the Mei-yu season in 2003. *Adv. Atmos. Sci.* **27**: 1193–1209.

Trenberth KE. 1998. Atmospheric moisture residence times and cycling: Implications for rainfall rates and climate change. *Clim. Change* **39**(4): 667–694.

Trenberth KE. 2011. Changes in precipitation with climate change. *Clim. Res.* **47**(1): 123–138.

Trenberth KE, Dai A, Rasmussen RM, Parsons DB. 2003. The changing character of precipitation. *Bull. Am. Meteorol. Soc.* **84**(9): 1205–1217.

Trenberth KE, Fasullo JT, Shepherd TG. 2015. Attribution of climate extreme events. *Nat. Clim. Change* **5**: 725–730, doi: 10.1038/NCLIMATE2657.

Utsumi N, Seto S, Kanae S, Maeda EE, Oki T. 2011. Does higher surface temperature intensify extreme precipitation? *Geophys. Res. Lett.* **38**: L16708, doi: 10.1029/2011GL048426.

Villarini G, Smith JA, Vecchi GA. 2013. Changing frequency of heavy rainfall over the central United States. *J. Clim.* **26**(1): 351–357.

Voss R, May R, Roeckner E. 2002. Enhanced resolution modelling study on anthropogenic climate change: changes in extremes of the hydrological cycle. *Int. J. Climatol.* **22**: 755–777.

Wang A, Fu J. 2013. Changes in daily climate extremes of observed temperature and precipitation in China. *Atmos. Ocean. Sci. Lett.* **6**(5): 312–319.

Wang X, Wu L, Ren F, Wang Y, Li W. 2008. Influences of tropical cyclones on China during 1965–2004. *Adv. Atmos. Sci.* **25**(3): 417–426.

Wang A, Lettenmaier D, Sheffield J. 2011. Soil moisture drought in China, 1950–2006. *J. Clim.* **24**(13): 3257–3271.

Wang W, Shao Q, Yang T, Peng S, Yu Z, Taylor J, Xing W, Zhao C, Sun F. 2013. Changes in daily temperature and precipitation extremes in the Yellow River Basin, China. *Stoch. Environ. Res. Risk Assess.* **27**(2): 401–421.

Wen G, Huang G, Hu K, Qu X, Tao W, Gong H. 2014. Changes in the characteristics of precipitation over northern Eurasia. *Theor. Appl. Climatol.* **119**: 653–665, doi: 10.1007/s00704-014-1137-8.

Westra S, Sisson SA. 2011. Detection of non-stationarity in precipitation extremes using a max-stable process model. *J. Hydrol.* **406**: 119–128.

Westra S, Alexander L, Zwiers F. 2013. Global increasing trends in annual maximum daily precipitation. *J. Clim.* **26**(11): 3904–3918.

Westra S, Fowler H, Evans JP, Alexander LV, Berg P, Johnson F, Kendon EJ, Lenderink J, Roberts NM. 2014. Future changes to the intensity and frequency of short-duration extreme rainfall. *Rev. Geophys.* **52**(3): 522–555.

Yang L, Villarini G, Smith JA, Tian F, Hu H. 2013. Changes in seasonal maximum daily precipitation in China over the period 1961–2006. *Int. J. Climatol.* **33**(7): 1646–1657.

Yao C, Yang S, Qian W, Lin Z, Wen M. 2008. Regional summer precipitation events in Asia and their changes in the past decades. *J. Geophys. Res.* **113**: D17107, doi: 10.1029/2007jd009603.

Yu R, Wang B, Zhou T. 2004. Climate effects of the deep continental stratus clouds generated by the Tibetan Plateau. *J. Clim.* **17**(13): 2702–2713.

Yu R, Xu Y, Zhou T, Li J. 2007a. Relation between rainfall duration and diurnal variation in the warm season precipitation over central eastern China. *Geophys. Res. Lett.* **34**(13): L13703, doi: 10.1029/2007gl030315.

Yu R, Zhou T, Xiong A, Zhu Y, Li J. 2007b. Diurnal variations of summer precipitation over contiguous China. *Geophys. Res. Lett.* **34**: L01704, doi: 10.1029/2006GL028129.

Yu R, Li J, Yuan W, Chen H. 2010. Changes in characteristics of late-summer precipitation over eastern China in the past 40 years revealed by hourly precipitation data. *J. Clim.* **23**(12): 3390–3396.

Zhai P, Pan X. 2003. Change in extreme temperature and precipitation over northern China during the second half of the 20th century. *Acta Geogr. Sin.* **58**: 1–10 (in Chinese).

Zhai P, Zhang X, Wan H, Pan X. 2005. Trends in total precipitation and frequency of daily precipitation extremes over China. *J. Clim.* **18**(7): 1096–1108.

Zhang X, Cong Z. 2014. Trends of precipitation intensity and frequency in hydrological regions of China from 1956 to 2005. *Glob. Planet. Change* **117**: 40–51, doi: 10.1016/j.gloplacha.2014.03.002.

Zhang H, Zhai P. 2011. Temporal and spatial characteristics of extreme hourly precipitation over eastern China in the warm season. *Adv. Atmos. Sci.* **28**(5): 1177–1183.

Zhang X, Zhang Z. 1979. A preliminary discussion on the northern boundary of subtropical zone in China: based on the distribution of broadleaf woody evergreens on the Qin-Lin Mountain. *Acta Geogr. Sin.* **34**(4): 342–352 (in Chinese).

Zhang Q, Liu Q, Wu L. 2009. Tropical cyclone damages in China 1983–2006. *Bull. Am. Meteorol. Soc.* **90**(4): 489–495.

Zhang Q, Singh VP, Li J, Chen X. 2011a. Analysis of the periods of maximum consecutive wet days in China. *J. Geophys. Res.* **116**: D23106, doi: 10.1029/2011JD016088.

Zhang X, Alexander L, Hegerl G, Jones P, Tank A, Peterson T, Trewin B, Zwiers F. 2011b. Indices for monitoring changes in extremes based on daily temperature and precipitation data. *WIREs Clim. Change* **2**(6): 851–870.

Zhang J, Liu X, Tan Z, Chen Q. 2012. Mapping of the north–south demarcation zone in China based on GIS. *J. Lanzhou Univ. (Nat. Sci.)* **48**(3): 28–33 (in Chinese).

Zhao T, Dai A, Wang J. 2012. Trends in tropospheric humidity from 1970 to 2008 over China from a homogenized radiosonde dataset. *J. Clim.* **25**(13): 4549–4567.

Zheng F, Westra S, Leonard M. 2015. Opposing local precipitation extremes. *Nat. Clim. Change* **5**(5): 389–390.

Zolina O, Simmer C, Gulev SK, Kollet S. 2010. Changing structure of European precipitation: Longer wet periods leading to more abundant rainfalls. *Geophys. Res. Lett.* **37**(6): L06704, doi: 10.1029/2010gl042468.

